FORCINN: First-order reversal curve inversion of magnetite using neural networks

Zhaowen Pei[1,2], Wyn Williams[1], Lesleis Nagy[3], Greig A. Paterson[3], Roberto Moreno[1,4], Adrian R. Muxworthy[5,6], and Liao Chang[2]

[1]School of GeoSciences, The University of Edinburgh, Edinburgh, UK
[2]Laboratory of Orogenic Belts and Crustal Evolution, School of Earth and Space Sciences, Peking University, Beijing, P. R. China
[3]Department of Earth, Ocean and Ecological Sciences, The University of Liverpool, Liverpool, UK
[4]CONICET, Instituto de Física Enrique Gaviola (IFEG), Córdoba, Argentina
[5]Department of Earth Science and Engineering, Imperial College London, London, UK
[6]Department of Earth Sciences, University College London, London, UK

Key Points:

- We have developed a neural network model for analyzing FORC data, which converges quickly to a high accuracy during the training.
- The trained FORCINN model can accurately invert the grain-size and aspect ratio distributions of simulated non-interacting magnetite FORCs.
- The trained FORCINN model performs well on inverting natural samples with a good estimate of grain-size distributions.

Corresponding author: Z. Pei and W. Williams, `zwpei@pku.edu.cn; wyn.williams@ed.ac.uk`

Abstract

First-order reversal curve (FORC) diagrams are a standard rock magnetic tool for analyzing bulk magnetic hysteresis behaviors, which are used to estimate the magnetic mineralogies and magnetic domain states of grains within natural materials. However, the interpretation of FORC distributions is challenging due to complex domain-state responses, which introduce well-documented uncertainties and subjectivity. Here, we propose a neural network algorithm (FORCINN) to invert the size and aspect ratio distribution from measured FORC data. We trained and tested the FORCINN model using a dataset of synthetic numerical FORCs for single magnetite grains with various grain-sizes (45-400 nm) and aspect ratios (oblate and prolate grains). In addition to successfully testing FORCINN against synthetic datasets, we also tested FORCINN against FORC data measured on natural samples with accurately determined grain-size and aspect ratio distributions. FORCINN was found to provide good estimates of the grain-size distributions for basalt samples and marine sediments.

Plain Language Summary

Magnetic minerals found in paleomagnetic and environmental samples are typically sub-micron or micron in size, rendering direct observation challenging. Therefore, to determine the grain-size properties, it has been standard practice for many decades to magnetically measure bulk samples, and to interpret their response in terms of the grain-size magnetic characteristics. One of the most sophisticated methods is the first-order reversal curve (FORC) diagram, which measures the change in net magnetization in a varying external field. However, FORC diagrams can be complex for natural samples and interpretation remains largely qualitative. This study proposes a machine-learning approach (FORCINN) to determine the size and aspect ratio of magnetite grains from FORC distributions. A large numerical dataset of FORC diagrams is simulated for magnetite grains of differing sizes and aspect ratios and is used to train the FORCINN model. We show that this model effectively estimates the size distribution of magnetite grains in natural specimens. As datasets encompassing diverse magnetic minerals are developed, this machine learning-based FORC inversion technique is anticipated to advance the macroscopic interpretations of magnetic mineral assemblages.

1 Introduction

First-order reversal curve (FORC) diagrams are a standard magnetic tool used to characterize the magnetic grains within samples, providing insights into their magnetic domain state and grain-size, their magnetic anisotropy and mineral composition, plus the degree of magnetostatic interactions within a rock (Roberts et al., 2000, 2022). FORC diagrams are constructed from partial magnetic-hysteresis loop data, by taking the mixed second derivative of the magnetization (Pike et al., 1999; Roberts et al., 2014). FORC data have been used in many geological and environmental studies to quantify paleo-environmental changes (e.g., Chang et al., 2018; Channell et al., 2016) and mineral-alteration processes (e.g., Chang, Pei, et al., 2023; Roberts et al., 2018). FORC data have also been used to determine paleomagnetic recording fidelity by determining the size and morphology of the constituent magnetic grains (Carvallo et al., 2006; Paterson et al., 2010). However, the interpretation of FORC data still remains problematic due to our incomplete understanding of how individual domain-state FORC signals combine and contribute to the total FORC distribution. The current approach of interpreting FORC observations involves qualitative comparisons with published analytical (e.g., Newell, 2005), experimental (e.g., Krása et al., 2011; Zhao et al., 2017) and numerical FORC distributions (e.g., Amor et al., 2022; Carvallo et al., 2003; Harrison & Lascu, 2014) for various magnetic domain structures. More complex analysis methods have been employed, e.g., principal component analysis (PCA) (Harrison et al., 2018; Lascu et al., 2015); however, these methods help to identify differences within datasets without explaining the underlying mechanisms.

A quantitative method is required to invert FORC data of natural samples to determine the magnetic grain size and morphology distribution. To achieve this we need detailed knowledge of the FORC response of grains as a function of grain-size and shape. Due to the difficulties in experimentally isolating the magnetic response of individual grain-sizes, forward micromagnetic modeling is key to solving this problem. There has been a long history of using forward micromagnetic simulations to study the FORC response of individual grains (e.g., Carvallo et al., 2003; Valdez-Grijalva et al., 2018) and interacting clusters (e.g. Bai et al., 2021; Harrison & Lascu, 2014; Muxworthy et al., 2004; Valdez-Grijalva et al., 2020); however, most of these forward models are limited in scope. In this work, we use the Synth-FORC dataset (Nagy et al., 2024), which comprises over a thousand numerically calculated magnetite FORCs, with each simulated grain having a different size and aspect ratio. These simulations, calculated using the MERRILL (Ó Conbhuí et al., 2018) micromagnetic software package, are combined with a machine learning approach that can directly estimate the size and morphology distribution of non-interacting magnetite grains from experimentally measured FORC distributions. This new tool is called FORCINN (FORC Inversion using Neural Networks).

2 Methods

The FORC distribution, represented as a two-dimensional matrix similar to an image (Berndt & Chang, 2019), has prompted us to explore the application of classical machine learning-based computer vision algorithms for FORC inversion. Convolutional neural networks (CNNs) are a classic algorithm for image processing, capable of effectively capturing fundamental features of images with rapid convergence and easy generalization (LeCun et al., 1998). ResNet improves upon CNNs by allowing deeper networks to extract more complex features (He et al., 2016). Hence, we constructed the FORCINN framework, utilizing two neural network-based machine learning algorithms, CNN and

ResNet, to invert FORC data and determine the distribution of grain-sizes and shapes (aspect ratio) of the magnetite assemblages in a sample (Figure 1). These models were trained us ing an extended Synth-FORC dataset described below, and tested against both synthetic and natural FORC data.

2.1 Training and testing dataset

The extended Synth-FORC dataset comprises micromagnetically generated FORCs for randomly-oriented magnetite grains with sizes varying between 45 and 195 nm equivalent spherical volume diameter (ESVD), and aspect ratios between 0.125 and 6.0 (Nagy et al., 2024). These grains have prolate (aspect ratio > 1) and oblate (aspect ratio < 1) shapes. Additional grain-sizes of 240 nm, 280 nm, 320 nm, and 400 nm (ESVD) were included, with the same aspect ratios as reported in Nagy et al. (2024). We utilized both lognormal and random distributions to sample size and shape distributions. Specifically, we generated a lognormal distribution by selecting various shape and scale parameters, and a random distribution by choosing different interval boundaries. These distributions were subsequently employed to synthesize the corresponding FORC samples. These distributions were subsequently used to synthesize the corresponding FORC samples. Our training data consisted of 400,000 FORCs; our testing set consisted of 100,000 FORCs. Both datasets were derived from Synth-FORC and sampled in the same way. All FORC data used in this study are normalized raw FORC magnetization M/M_s, along with additional finite difference approximations of $\partial(M/M_s)/\partial B_r$, $\partial(M/M_s)/\partial B$ and $\partial^2(M/M_s)/\partial B_r \partial B$, where M is magnetization at field B with reversal field B_r, normalized by the saturation magnetization M_s. We also include a white noise signal-component accounting for 5%, 10%, and 20% of magnetization to evaluate the robustness of our models.

In addition to testing the model against the synthetic test data, FORCINN was evaluated against five experimental FORC datasets where the grain morphology distributions were independently measured. These datasets consist of two basalt samples previously studied (Michalk et al., 2008; Muxworthy, 2010; Muxworthy et al., 2011): one from the 1991 C.E. Hekla (Iceland) eruption (sample code HB91CY), and the other from the 1944 C.E. Vesuvius (Italy) eruption (VM1AX), with grain geometries recently determined using focused-ion beam nanotomography (FIB-nt) (Gergov et al., 2024). Two marine sediment samples (MD2361-125 and MD2361-315) from the core MD00-2361 from offshore North West Cape (Western Australia) were included, with dimension data determined through transmission electron microscopy (TEM) (Chang, Hoogakker, et al., 2023). Finally, a synthetic Wright magnetite powder sample (W(0.3 µm)) with grain dimension data obtained via scanning electron microscopy (Muxworthy & Dunlop, 2002), was also used to test FORCINN.

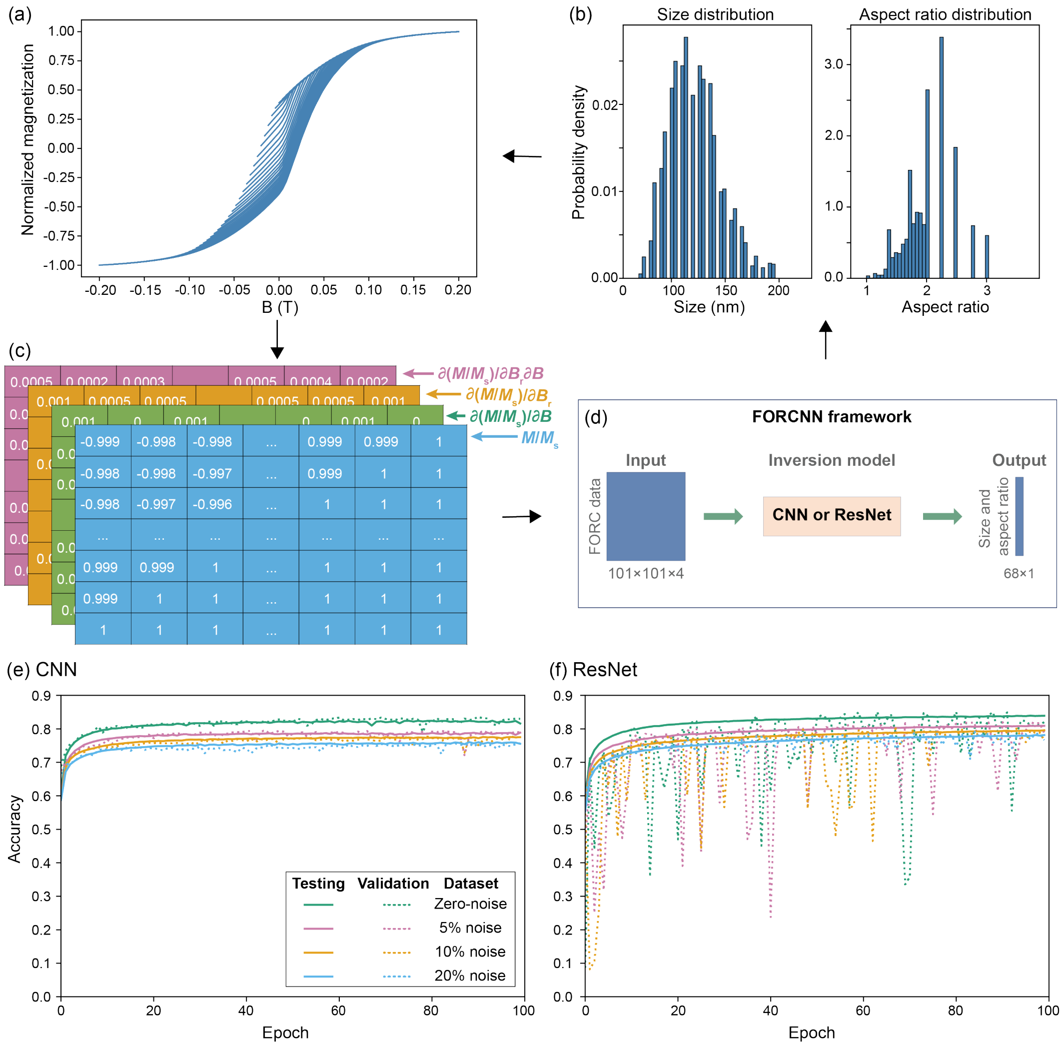

Figure 1. Framework for FORC inversion based on neural networks (FORCINN) and training accuracy. (a) The original FORC data. (b) The corresponding size and aspect ratio distribution used to determine (a). (c) The input for the FORCINN model, including the original normalized FORC magnetization M/M_s, and its first-order derivatives ($\partial(M/M_s)/\partial B_r$ and $\partial(M/M_s)/\partial B$) and second-order derivatives ($\partial^2(M/M_s)/\partial B_r \partial B$). (d) The inversion framework of the FORCINN using CNN and ResNet models. Training results of CNN (e) and ResNet models (f) trained with zero-noise, 5% noise, 10% noise, and 20% noise, including the accuracy of the training set (solid lines) and the validation set (dashed lines).

2.2 Model construction

FORC inversion is a multi-regression problem where the input variable is the set of major and minor hysteresis loops that make up a FORC-diagram (Figure 1a), and the output variables are the size and aspect ratio distributions. To ensure efficient model convergence, we simplify the output variable to a histogram that represents the corresponding size and shape distribution (Figure 1b): the size range of the output histogram (from 45 nm to 400 nm) is split into 35 bins, and the aspect ratio range (from 0.166667 to 6.0) is split into 33 bins. In other words, we simplified the FORC inversion from a multi-regression problem to a multi-class classification problem. Hence, the model output layer is a SoftMax activation function (Bridle, 1989) consisting of a $1\times$ 68 vector, representing the fractional contributions of size (35 bins) and aspect ratio (33 bins).

Each input value in our dataset is encoded as an array of four two-dimensional 'slabs' ($101 \times 101 \times 4$; Figure 1c). The horizontal index of each slab corresponds to the B_r field ranging from -0.2 T to 0.2 T in steps of 0.004 T plus additional one-padding values – resulting in 101 sample points; this is the same for the vertical index of each slab that corresponds to the B field. We include one-padding values due to the triangular array structure that FORCs are measured (see Figure 1 in Nagy et al. (2024) for reference), where only the row corresponding to the major hysteresis loop is fully populated. Each slab (indexed from 0 to 3) is derived from raw FORC magnetization: the first slab is the magnetization normalized by the saturation value M_s; slabs 1-3 are finite difference approximations of the two first and mixed second partial derivatives of the normalized magnetization.

Neural network algorithms contain a number of hidden layers that non-linearly connect (map) the input and output (Rumelhart et al., 1986). The hidden layers of CNN model mainly consist of convolutional layers and max-pooling layers (Figure S1 and Table S1), which extract features from images through local connections and weight sharing (LeCun et al., 2015). ResNet introduces residual blocks based on CNN, which add shortcut connections to address the vanishing gradient problem in deep networks (Figure S2 and Tables S2 and S3), making it possible to train deeper networks (He et al., 2016). The detailed descriptions of the hidden layers in CNN and ResNet can be found in Supporting Information Text S1.

2.3 Training and Testing Process

We adopted 75% of the training set for training and 25% for validation. The training dataset is divided into batches of size 32 during training, with each batch used to train the model in one iteration (Chollet, 2021). An epoch is a complete pass of the learning algorithm over the entire training dataset (Chollet, 2021). The model was trained for a total of 100 epochs. To evaluate the model convergence performance, we recorded the training accuracy, defined as the proportion of samples for which the model correctly predicted the highest probability class (Chollet, 2021). Finally, the trained model was then tested on the testing set to evaluate its generalization ability.

3 Training and Testing on Simulation Datasets

Figures 1e and 1f show the accuracies of the CNN and ResNet algorithms on zero-noise, 5% noise, 10% noise, and 20% noise datasets after 100 epochs of training. The accuracies for the testing data set converged to approximately the same level, i.e., 82%, 79%, 77%, and 76%, respectively for the CNN model; and 84%, 81%, 79%, and 78%, respectively for the ResNet model. The accuracy of the CNN model on the validation set is similar to that on the training set, whereas the validation accuracy of the ResNet model shows significant fluctuations, which may be due to the higher complexity of ResNet. For both networks, training accuracy slightly decreases with increasing noise.

When applied to the simulation testing set, CNN models trained with zero-noise, 5% noise, 10% noise, and 20% noise datasets consistently deliver precise predictions of the average size and aspect ratio, as indicated by $R^2 > 0.98$ (Figures 2a-2h). The predictive performance of the ResNet models trained with the high noise dataset is poorer, but still achieves $R^2 > 0.79$ for size and >0.94 for the aspect ratio. Figure 3 shows a clear correlation between the ground truth and predicted distributions of size and aspect ratio for the CNN model trained with the zero-noise dataset, with $R^2 > 0.85$. These results on synthetic FORCs indicate that well-trained CNN and ResNet models have the potential to generalize to the size and aspect ratio inversion from the FORC distribution observations on non-interacting magnetite.

4 Testing on the Experiment Data

4.1 Testing results

The well-trained FORCINN model was used to invert the experimental FORC data of four natural samples and one synthetic powder sample (Figure 4). The FORC inversion results of the basalt samples from Helka and Vesuvius exhibit similar size distributions as those determined from FIB-nt with p-values >0.05 of Kolmogorov-Smirnov test (Dodge, 2008) (Figures 4a and 4c). The experimentally determined mean/median for the Hekla sample was ∼88/71 µm versus a prediction of ∼111/100 µm, and for Vesuvius an experimental estimate of ∼174/136 µm versus a prediction of ∼147/120 µm. In both cases the predicted size distribution underestimates the grain content in the <80 nm range. This is likely due to relatively small variations in the hysteresis responses for grains in the single domain (SD) range, i.e., 45-85 nm for equant grains (Williams & Dunlop, 1989; Nagy et al., 2024). The predicted aspect-ratio distributions are relatively narrower compared to the experimental data (Figures 4b and 4d), in particular the number of oblate particles is underestimated.

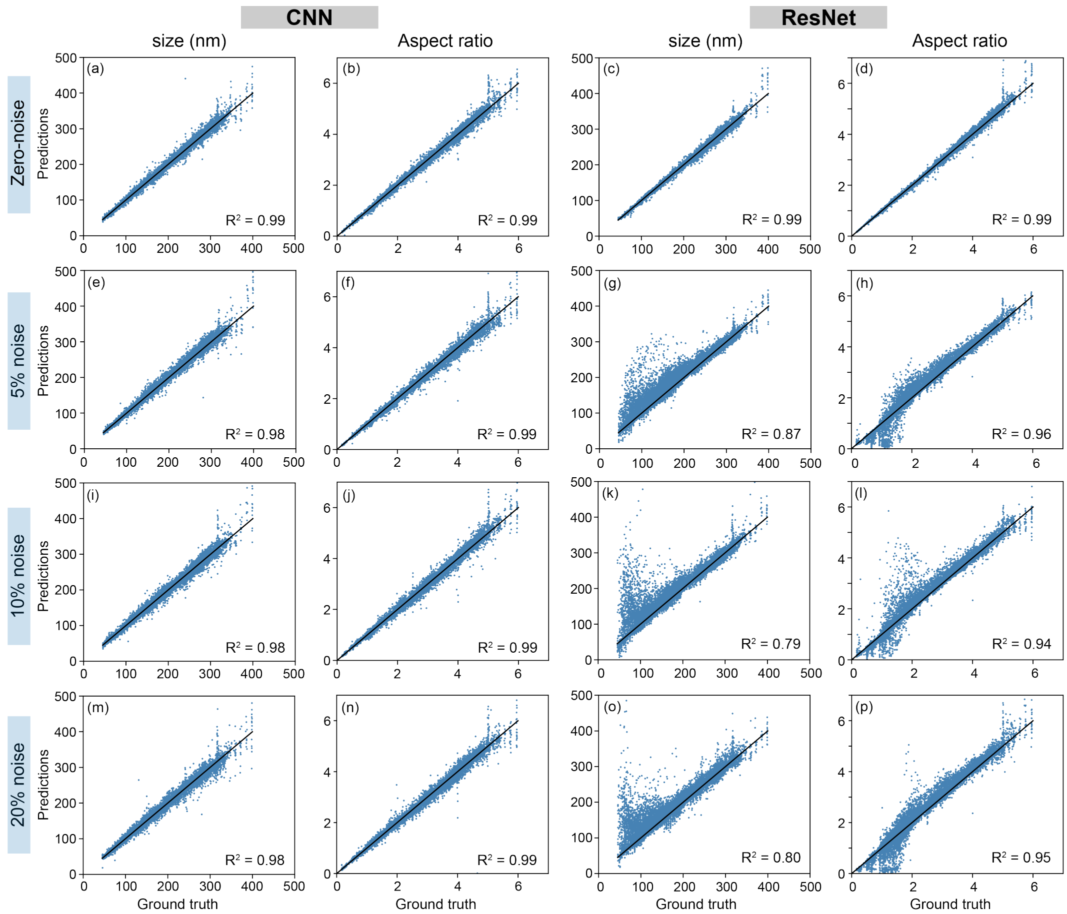

Figure 2. FORCINN predicted versus ground truth for the simulation dataset of CNN (a, b, e, f, i, j, m, n) and ResNet (c, d, g, h, k, l, o, p) models trained with zero-noise, 5% noise, 10% noise, and 20% noise datasets, including ground truth and predicted average of sizes (a, c, e, g, i, k, m, o) and aspect ratio (b, d, f, h, j, l, n, p) distributions. The black line represents where the ground truth and predictions are equal. Coefficient of determination R^2 represents the goodness of fit of the model (Draper, 1998).

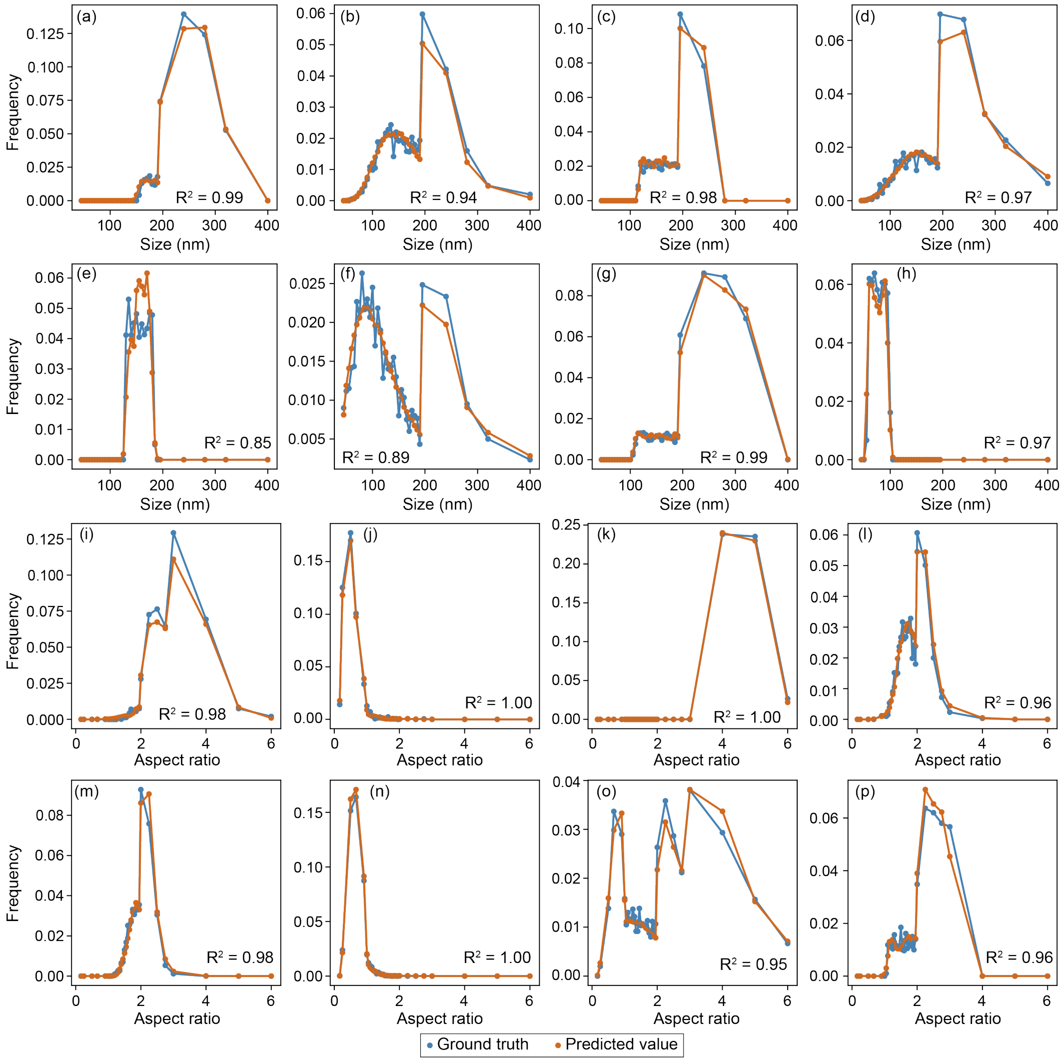

Figure 3. Frequency versus grain-size (a-h) or aspect ratio (i–p) for the input distribution for the synthetic ground truth FORC data (blue lines and dots) and the FORCINN predicted distribution (orange lines and dots). The prediction results are for the CNN model trained with the zero-noise dataset. Coefficient of determination R^2 represents the goodness of fit of the model (Draper, 1998).

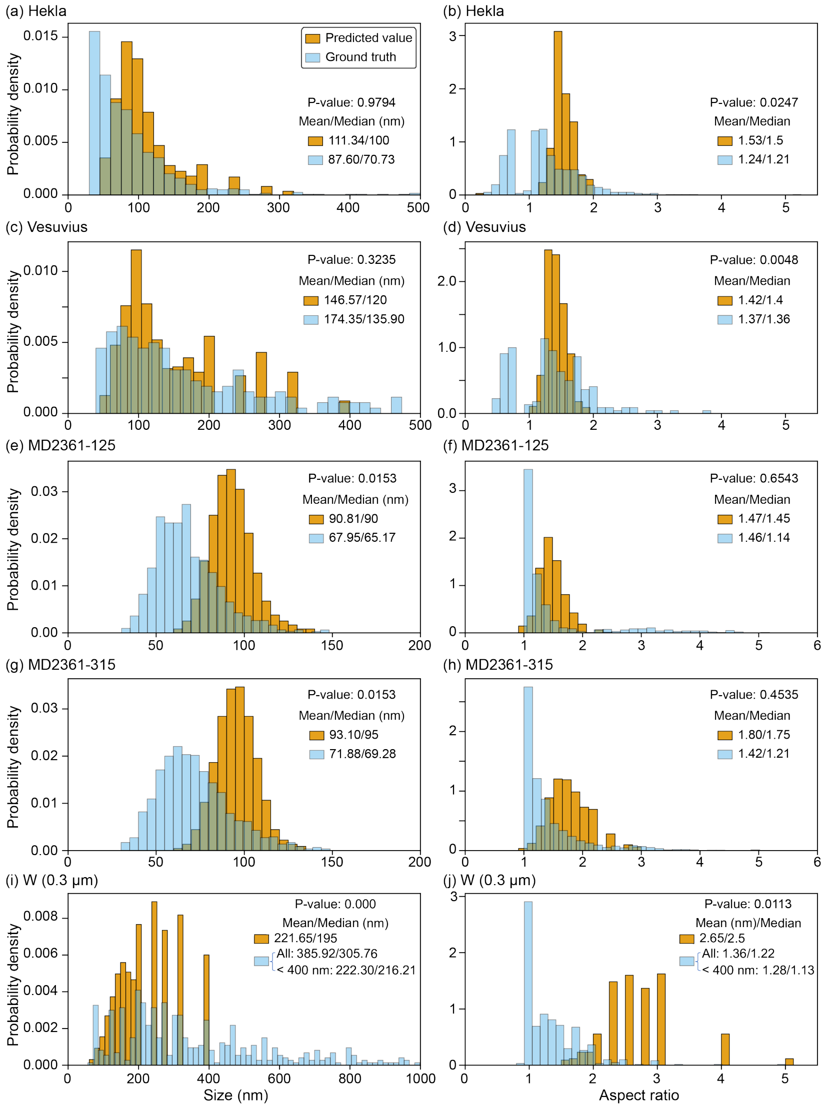

Figure 4. Probability density versus grain-size (a, c, e, g, i) or aspect ratio (b, d, f, h, j) for the FORCINN predicted (orange) and the experimental ground truth data (blue). The experimental data are for (a, b) Hekla, (c, d) Vesuvius, (e, f) MD2361-125, (g, h) MD2361-315, and (i, j) Wright powder sample W(0.3 µm). For the Hekla and Vesuvius samples the distributions were determined via FIB-nT (Gergov et al., 2024), whereas for MD2361-125, MD2361-315 and W(0.3 µm), the grain-size distributions are determined from 2D images (Chang, Hoogakker, et al., 2023; Muxworthy & Dunlop, 2002). P-values were calculated by Kolmogorov-Smirnov test (Williams & Dunlop, 1989; Nagy et al., 2024), which can indicate that the null hypothesis that the two data distributions are indistinguishable cannot be rejected if greater than 0.05. The prediction results of all models are presented in Tables S4-S8. This figure shows the results of the model with the best overall predictive performance, characterized by a large p-value and mean/median values close to the experimental data, specifically the ResNet model trained with 20% noise dataset (a-h) and the CNN model trained with zero-noise dataset (i and j). The mean and median are marked in the figure.

In general, there are a number of other reasons why the predicted distributions do not match the experimental data: (1) the experimental FORC data were acquired on bulk samples (~1 cm^3), which likely include wider grain-size distributions than the experimentally determined grain-size distributions, which are from much smaller volumes of sample, i.e, $\sim 10^{-6}$ cm^3. (2) There maybe magnetostatic interactions in the experimental data; however, for the basalt samples they are thought to be minimal (Gergov et al., 2024). (3) The FORC training data only extends to 400 nm in size. (4) The morphologies of the real magnetic grains are more complex than the numerical models. The training dataset only considers grains with equal intermediate and minor axes, while the reconstructed data has three different main axes. Despite some limitations in the dataset and predictions, the current testing results have sufficiently demonstrated the potential of FORCINN in inverting FORC data of basalt samples. These inverted morphological data can be utilized to evaluate the reliability of basalt paleointensity data (e.g., Carvallo et al., 2006; Nagy et al., 2022).

The predicted size distributions of two marine sediment samples containing magnetofossils are larger than the size distribution obtained from the TEM image (Figures 4e and 4g). The predicted aspect ratios are also higher (Figures 4f and 4h). These differences may be because only the morphological data of magnetofossils were counted from TEM images, excluding the larger detrital magnetite in the sample (Chang, Hoogakker, et al., 2023). Furthermore, some magnetofossils in sediments may also retain chain structures (Amor et al., 2022), which exhibit strong interactions and result in an overestimation of inverted grain-size and aspect ratio. However, the inverted results correctly identified that the size and high aspect ratio component of the glacial sediment sample (MD2361-315) are both larger than those of the interglacial sample (MD2361-125; Figures 4e-4h). These size and aspect ratio variations are thought to be indicative of past ocean oxygen changes (Chang, Hoogakker, et al., 2023).

For the Wright powder sample, the grain-size mean/median predicted by FORCINN (~222/195 µm) is smaller than the measured values of ~386/306 µm (Figure 4i). This difference is likely due to the training dataset only extending to 400 nm; whilst the sample has many grains >400 nm. Additionally, this powder sample was reported by Muxworthy and Dunlop (2002) to contain magnetostatically interacting grains with angular geometries, which would both contribute to the differences seen in Figure 4i. Mismatches between the measured and predicted aspect ratios for the Wright powder sample are also seen (Figure 4j). As the micromagnetic data set of simulated FORCs expands to encompass larger grains with more diverse shapes, we expect this mismatch to greatly improve.

4.2 Implications for rock, environmental, and paleo- magnetism

The ability to accurately estimate the magnetic grain-size distributions like we have achieved on five experimental FORC data using FORCINN (Figure 4), has been a long-standing problem in the magnetism community. Previous methods have focused on determining coercivity distributions (e.g., Kruiver et al., 2001; Maxbauer et al., 2016), unmixing to produce end-members, which themselves contain complex distributions (e.g. Heslop & Dillon, 2007; Harrison et al., 2018), or have been based purely on single-domain theory, which limits their usefulness (e.g, Dunlop, 1976; Shcherbakov & Fabian, 2005). FORCINN is the first method capable of rapidly inverting rapidly measured magnetic data for their grain-size distribution, for grains that are larger than single-domain. FORCINN marks a major breakthrough in rock magnetic analysis with applications in areas of rock, environmental, and paleo- magnetism. Clearly, the training dataset needs to be extended to include larger grain-sizes plus different mineralogies for which micromagnetic models have already been made, e.g., greigite (Valdez-Grijalva et al., 2018). Ideally, magnetostatic interactions should also be included, but this is more challenging for magnetic particles, which display non-uniform magnetic behavior due to computational limits (Valdez-Grijalva et al., 2020), and it is thought that in many natural samples magnetostatic interactions are not significant (Muxworthy, 2013).

5 Conclusions

We have developed a neural network-based FORC inversion model (FORCINN) that accurately predicts the size and aspect ratio distribution of non-interacting magnetite from their measured FORC distributions. The trained FORCINN model achieves precise predictions on a testing FORC dataset generated from micromagnetic simulations of individual magnetite grains (Figures 2 and 3). FORCINN also shows promise in inverting FORC data for their grain-size and aspect ratio distributions of five experimental datasets, for which the grain morphology information had been previously determined independently using electron microscopic methods (Figure 4).

FORCINN provides CNN and ResNet models trained at different noise levels for comparison. For the micromagnetically generated non-interacting magnetite testing set, CNN outperforms ResNet with higher goodness of fit. For natural basalt and marine sediment samples, the ResNet model trained on the 20% noise dataset demonstrated the best performance. Therefore, we recommend trying this model first for inverting natural samples.

The current training dataset only includes FORC data from single magnetite with sizes ranging from 45 to 400 nm and aspect ratios from 0.166667 to 6, and lacks grains that exhibit triaxial morphological differences. This limits the inversion capability on FORC data of complex natural samples. In the future, it is important to expand the current dataset to include larger grain-sizes, a broader range of minerals, and potentially magnetostatic interactions.

Open Research

The data and code related to this study have been uploaded to the Zenodo repository (Pei et al., 2024), which includes the codes for building, training, and testing the FORCINN model, dataset processing codes, trained CNN and ResNet models, and the raw data for the testing and training sets.

Acknowledgments

Z.P. acknowledges the support of the China Scholarship Council program (202306010245) for sponsoring his visit to the University of Edinburgh. W.W. and A.R.M. acknowledge Natural Environment Research Council (NERC) for their financial support (NE/S001018/1). G.A.P. acknowledges funding from NERC grants NE/W006707/1 and NE/Y005686/1. R.M acknowledges the posdoctoral funding scheme of Conicet, Argentina.

References

Amor, M., Wan, J., Egli, R., Carlut, J., Gatel, C., Andersen, I. M., ... Komeili, A. (2022). Key signatures of magnetofossils elucidated by mutant magnetotactic bacteria and micromagnetic calculations. *Journal of Geophysical Research: Solid Earth*, *127*(1), e2021JB023239.

Bai, F., Chang, L., Berndt, T. A., & Pei, Z. (2021). Micromagnetic calculations of the effect of magnetostatic interactions on isothermal remanent magnetization curves: Implications for magnetic mineral identification. *Journal of Geophysical Research: Solid Earth*, *126*(7), e2021JB022335.

Berndt, T. A., & Chang, L. (2019). Waiting for forcot: Accelerating forc processing 100× using a fast-fourier-transform algorithm. *Geochemistry, Geophysics, Geosystems*, *20*(12), 6223–6233.

Bridle, J. (1989). Training stochastic model recognition algorithms as networks can lead to maximum mutual information estimation of parameters. *Advances in neural information processing systems*, *2*.

Carvallo, C., Muxworthy, A. R., Dunlop, D. J., & Williams, W. (2003). Micromagnetic modeling of first-order reversal curve (forc) diagrams for single-domain and pseudo-single-domain magnetite. *Earth and Planetary Science Letters*, *213*(3-4), 375-390. doi: 10.1016/S0012-821X(03)00320-0

Carvallo, C., Roberts, A. P., Leonhardt, R., Laj, C., Kissel, C., Perrin, M., & Camps, P. (2006). Increasing the efficiency of paleointensity analyses by selection of samples using first-order reversal curve diagrams. *Journal of Geophysical Research-Solid Earth*, *111*(B12), B12103. doi: 10.1029/2005JB004126

Chang, L., Harrison, R. J., Zeng, F., Berndt, T. A., Roberts, A. P., Heslop, D., & Zhao, X. (2018). Coupled microbial bloom and oxygenation decline recorded by magnetofossils during the palaeocene–eocene thermal maximum. *Nature Communications*, *9*(1), 4007.

Chang, L., Hoogakker, B. A., Heslop, D., Zhao, X., Roberts, A. P., De Deckker, P., ... others (2023). Indian ocean glacial deoxygenation and respired carbon accumulation during mid-late quaternary ice ages. *Nature Communications*, *14*(1), 4841.

Chang, L., Pei, Z., Xue, P., Wang, S., Wang, Z., Krijgsman, W., & Dekkers, M. J. (2023). Self-reversed magnetization in sediments caused by greigite alteration. *Geophysical Research Letters*, *50*(12), e2023GL103885.

Channell, J., Harrison, R., Lascu, I., McCave, I., Hibbert, F., & Austin, W. E. (2016). Magnetic record of deglaciation using forc-pca, sortable-silt grain size, and magnetic excursion at 26 ka, from the rockall trough (ne atlantic). *Geochemistry, Geophysics, Geosystems*, *17*(5), 1823–1841.

Chollet, F. (2021). *Deep learning with python.* Simon and Schuster.

Dodge, Y. (2008). *The concise encyclopedia of statistics.* Springer New York.

Draper, N. (1998). *Applied regression analysis.* McGraw-Hill. Inc.

Dunlop, D. J. (1976). Thermal fluctuation analysis: a new technique in rock magnetism. *Journal of Geophysical Research*, *81*, 3511–3517. doi: 10.1029/JB081i020p03511

Gergov, H., Muxworthy, A., Williams, W., & Cowan, A. (2024, May). *Supplementary dataset for 'Magnetic recording fidelity of basalts through 3D nanotomography, 2024'.* Zenodo. doi: 10.5281/zenodo.11369780

Harrison, R. J., & Lascu, I. (2014). Forculator: A micromagnetic tool for simulating first-order reversal curve diagrams. *Geochemistry, Geophysics, Geosystems*, *15*(12), 4671–4691.

Harrison, R. J., Muraszko, J., Heslop, D., Lascu, I., Muxworthy, A. R., & Roberts, A. P. (2018). An improved algorithm for unmixing first-order reversal curve diagrams using principal component analysis. *Geochemistry, Geophysics, Geosystems*. doi: 10.1029/2018GC007511

He, K., Zhang, X., Ren, S., & Sun, J. (2016). Deep residual learning for image recognition. In *Proceedings of the ieee conference on computer vision and pattern recognition* (pp. 770–778).

Heslop, D., & Dillon, M. (2007). Unmixing magnetic remanence curves without a priori knowledge. *Geophys. J. Int.*(170), 556-566.

Krása, D., Muxworthy, A., & Williams, W. (2011). Room- and low-temperature magnetic properties of two-dimensional magnetite particle arrays. *Geophysical Journal International*, *185*, 167–180. doi: 10.1111/j.1365-246X.2011.04956.x

Kruiver, P. P., Dekkers, M. J., & Heslop, D. (2001). Quantification of magnetic coercivity components by the analysis of acquisition curves of isothermal remanent magnetisation. *Earth and Planetary Science Letters*, *189*(3), 269-276. doi: 10.1016/S0012-821X(01)00367-3

Lascu, I., Harrison, R. J., Li, Y., Muraszko, J. R., Channell, J. E. T., Piotrowski, A. M., & Hodell, D. A. (2015). Magnetic unmixing of first-order reversal curve diagrams using principal component analysis. *Geochemistry, Geophysics,* *Geosystems*, *16*, 2900-2915. doi: 10.1002/2015GC005909

LeCun, Y., Bengio, Y., & Hinton, G. (2015). Deep learning. *nature*, *521*(7553), 436–444.

LeCun, Y., Bottou, L., Bengio, Y., & Haffner, P. (1998). Gradient-based learning applied to document recognition. *Proceedings of the IEEE*, *86*(11), 2278–2324.

Maxbauer, D. P., Feinberg, J. M., & Fox, D. L. (2016). Max unmix: A web application for unmixing magnetic coercivity distributions. *Computers & Geosciences*, *95*, 140-145. doi: 10.1016/j.cageo.2016.07.009

Michalk, D. M., Muxworthy, A. R., Boehnel, H. N., Maclennan, J., & Nowaczyk, N. (2008). Evaluation of the multispecimen parallel differential ptrm method: a test on historical lavas from iceland and mexico. *Geophysical Journal International*, *173*(2), 409-420. doi: 10.1111/j.1365-246X.2008.03740.x

Muxworthy, A. R. (2010). Revisiting a domain-state independent method of palaeointensity determination. *Physics of the Earth and Planetary Interiors*, *179*(1-2), 21-31. doi: 10.1016/j.pepi.2010.01.003

Muxworthy, A. R. (2013). The role of magnetic interactions in natural systems. *Astronomy & Geophysics*, *54*(2), 2–31.

Muxworthy, A. R., & Dunlop, D. J. (2002). First-order reversal curve (FORC) diagrams for pseudo-single-domain magnetites at high temperature. *Earth and Planetary Science Letters*, *203*(1), 369-382. doi: 10.1016/S0012-821X(02)00880-4

Muxworthy, A. R., Heslop, D., Paterson, G. A., & Michalk, D. (2011). A Preisach method for estimating absolute paleofield intensity under the constraint of using only isothermal measurements: 2. Experimental testing. *Journal of Geophysical Research Solid Earth*, *116*, B04103. doi: 10.1029/2010JB007844

Muxworthy, A. R., Heslop, D., & Williams, W. (2004). Influence of magnetostatic interactions on first-order-reversal-curve (FORC) diagrams: a micromagnetic approach. *Geophysical Journal International*, *158*(3), 888-897. doi: 10.1111/j.1365-246X.2004.02358.x

Nagy, L., Moreno, R., Muxworthy, A. R., Williams, W., Paterson, G. A., Tauxe, L., & Valdez-Grijalva, M. A. (2024). Micromagnetic determination of the forc response of paleomagnetically significant magnetite assemblages. *Geochemistry, Geophysics, Geosystems*, *25*(7), e2024GC011465.

Nagy, L., Williams, W., Tauxe, L., & Muxworthy, A. R. (2022). Chasing tails: Insights from micromagnetic modeling for thermomagnetic recording in non-uniform magnetic structures. *Geophysical Research Letters*, *49*(23), e2022GL101032.

Newell, A. J. (2005). A high-precision model of first-order reversal curve (forc) functions for single-domain ferromagnets with uniaxial anisotropy. *Geochemistry Geophysics Geosystems*, *6*, Q05010. doi: 10.1029/2004GC000877

Ó Conbhuí, P., Williams, W., Fabian, K., Ridley, P., Nagy, L., & Muxworthy, A. R. (2018). Merrill: Micromagnetic earth related robust interpreted language laboratory. *Geochemistry, Geophysics, Geosystems*, *19*(4), 1080–1106.

Paterson, G. A., Muxworthy, A. R., Roberts, A. P., & Mac Niocaill, C. (2010). Assessment of the usefulness of lithic clasts from pyroclastic deposits for paleointensity determination. *Journal of Geophysical Research: Solid Earth*, *115*(B3).

Pei, Z., Williams, W., Nagy, L., Paterson, G., Moreno, R., Muxworthy, A., & Chang, L. (2024). *Code for 'FORCINN: First-order reversal curve inversion of magnetite using neural networks'.* Zenodo. doi: 10.5281/zenodo.13838980

Pike, C. R., Roberts, A. P., & Verosub, K. L. (1999). Characterizing interactions in fine magnetic particle systems using first order reversal curves. *Journal of Applied Physics*, *85*(9), 6660–6667.

Roberts, A. P., Heslop, D., Zhao, X., Oda, H., Egli, R., Harrison, R. J., ... Sato, T. (2022). Unlocking information about fine magnetic particle assemblages from first-order reversal curve diagrams: Recent advances. *Earth-Science Reviews*, *227*, 103950.

Roberts, A. P., Heslop, D., Zhao, X., & Pike, C. R. (2014). Understanding fine magnetic particle systems through use of first-order reversal curve diagrams. *Reviews of Geophysics*, *52*(4), 557–602. doi: 10.1002/2014RG000462

Roberts, A. P., Pike, C. R., & Verosub, K. L. (2000). First-order reversal curve diagrams: A new tool for characterizing the magnetic properties of natural samples. *Journal of Geophysical Research: Solid Earth*, *105*(B12), 28461–28475.

Roberts, A. P., Zhao, X., Harrison, R. J., Heslop, D., Muxworthy, A. R., Rowan, C. J., ... Florindo, F. (2018). Signatures of reductive magnetic mineral diagenesis from unmixing of first-order reversal curves. *Journal of Geophysical Research: Solid Earth*, *123*(6), 4500–4522.

Rumelhart, D. E., Hinton, G. E., & Williams, R. J. (1986). Learning representations by back-propagating errors. *nature*, *323*(6088), 533–536.

Shcherbakov, V. P., & Fabian, K. (2005). On the determination of magnetic grain-size distributions of superparamagnetic particle ensembles using the frequency dependence of susceptibility at different temperatures. *Geophysical Journal International*, *162*, 736-746. doi: 10.1111/j.1365-246X.2005.02603.x

Valdez-Grijalva, M. A., Muxworthy, A. R., Williams, W., Ó Conbhuí, P., Nagy, L., Roberts, A. P., & Heslop, D. (2018). Magnetic vortex effects on first-order reversal curve (FORC) diagrams for greigite dispersions. *Earth and Planetary Science Letters*, *501*, 103-111. doi: 10.1016/j.epsl.2018.08.027

Valdez-Grijalva, M. A., Nagy, L., Muxworthy, A. R., Williams, W., Roberts, A. P., & Heslop, D. (2020). Micromagnetic simulations of first-order reversal curve (FORC) diagrams of framboidal greigite. *Geophysical Journal International*, *222*(2), 1126-1134. doi: 10.1093/gji/ggaa241

Williams, W., & Dunlop, D. J. (1989). Three-dimensional micromagnetic modelling of ferromagnetic domain structure. *Nature*, *337*(6208), 634–637. doi: 10.1038/

337634a0

Zhao, X., Roberts, A. P., Heslop, D., Paterson, G. A., Li, Y., & Li, J. (2017). Magnetic domain state diagnosis using hysteresis reversal curves. *Journal of Geophysical Research: Solid Earth*, *122*(7), 4767–4789.